Journal of Alzheimer's Disease xx (2021) x–xx
DOI 10.3233/JAD-210308
IOS Press



# Amyloid Deposition Is Greater in Cerebral Gyri than in Cerebral Sulci with Worsening Clinical Diagnosis Across the Alzheimer's Disease Spectrum

Lucas M. Walden[a], Song Hu[a], Anant Madabhushi[c,d],
Jeffrey W. Prescott[a,b,*] and for the Alzheimer's Disease Neuroimaging Initiative[1]
[a]*MetroHealth, Department of Radiology, Cleveland, OH, USA*
[b]*Case Western Reserve University, School of Medicine, Cleveland, OH, USA*
[c]*Case Western Reserve University, Department of Biomedical Engineering, Center for Computational Imaging & Personalized Diagnostics, Cleveland, OH, USA*
[d]*Louis Stokes Cleveland VA Medical Center, Cleveland, OH, USA*

Accepted 19 June 2021
Pre-press 26 July 2021

**Abstract**.
**Background:** Histopathologic studies have demonstrated differential amyloid-β (Aβ) burden between cortical sulci and gyri in Alzheimer's disease (AD), with sulci having a greater Aβ burden.
**Objective:** To characterize Aβ deposition in the sulci and gyri of the cerebral cortex *in vivo* among subjects with normal cognition (NC), mild cognitive impairment (MCI), and AD, and to evaluate if these differences could improve discrimination between diagnostic groups.
**Methods:** T1-weighted 3T MR and florbetapir (amyloid) positron emission tomography (PET) data were obtained from the Alzheimer's Disease Neuroimaging Initiative (ADNI). T1 images were segmented and the cortex was separated into sulci/gyri based on pial surface curvature measurements. T1 images were registered to PET images and regional standardized uptake value ratios (SUVr) were calculated. A linear mixed effects model was used to analyze the relationship between clinical variables and amyloid PET SUVr measurements in the sulci/gyri. Receiver operating characteristic (ROC) analysis was performed to define amyloid positivity. Logistic models were used to evaluate predictive performance of clinical diagnosis using amyloid PET SUVr measurements in sulci/gyri.
**Results:** 719 subjects were included: 272 NC, 315 MCI, and 132 AD. Gyral and sulcal Aβ increased with worsening cognition, however there was a greater increase in gyral Aβ. Females had a greater gyral and sulcal Aβ burden. Focusing on sulcal and gyral Aβ did not improve predictive power for diagnostic groups.

[1]Data used in preparation of this article were obtained from the Alzheimer's Disease Neuroimaging Initiative (ADNI) data base (http://adni.loni.usc.edu). As such, the investigators within the ADNI contributed to the design and implementation of ADNI and/or provided data but did not participate in analysis or writing of this report. A complete listing of ADNI investigators can be found at: http://adni.loni.ucla.edu/wp-content/uploads/how_to_apply/ADNI_Acknowledgement_List.pdf

*Correspondence to: Jeffrey W. Prescott, MD, PhD, Assistant Professor, Department of Radiology, MetroHealth Medical Center, Academic Department of Radiology, Case Western Reserve University, 2500 MetroHealth Drive, Cleveland, OH 44109, USA. Tel.: +1 216 778 4880; E-mail: jprescott@metrohealth.org.

**Conclusion:** While there were significant differences in Aβ deposition in cerebral sulci and gyri across the AD spectrum, these differences did not translate into improved prediction of diagnosis. Females were found to have greater gyral and sulcal Aβ burden.

Keywords: Alzheimer's disease, amyloid PET imaging, gyral/gyri, sulcal/sulci

## INTRODUCTION

Histopathologic studies have demonstrated differential Aβ burden between cortical sulci and gyri in AD, with sulci having a greater average Aβ burden [1, 2]. Differential Aβ accumulation in sulci and gyri is thought to have an anatomic or cytoarchitectural basis [1, 2]. For instance, sulci are known to have a thicker supragranular layer, the layer most susceptible to Aβ deposition, and sulci have a higher cellular density [3]. In addition, overall thinning of cortical sulci may play a role in the differential Aβ accumulation especially when measuring Aβ as a percentage of the cortical layer [4]. Other possible explanations include altered blood supply, degenerative changes in cortical folding, and Aβ plaque morphology [4–6]. Several studies have detailed morphologic changes in sulci or gyri across the AD spectrum [7, 8]. For instance, greater sulcal widening, shallower sulcal depth, and reductions in gyral white matter volume have been identified with progression from NC to MCI and MCI to AD [8]. These changes could be secondary to aberrant Aβ accumulation and therefore examining Aβ burden in cortical sulci and gyri may result in early identification of pathologic Aβ accumulation and provide important discriminative information for those at increased risk for development of AD and associated cognitive decline. In addition, regional differences could translate into improved thresholding for classification of Aβ positivity, the importance of which has recently been highlighted with the proposal of a biological definition of AD, which incorporates imaging and biofluid measures of Aβ plaques, tau neurofibrillary tangles, and neurodegeneration, independent of clinical symptoms [9].

The aim of this study was to characterize the deposition of Aβ in the sulci and gyri of the neocortex *in vivo* among subjects along the spectrum of AD and to identify whether greater clinical differences could be identified by focusing on either gyral or sulcal Aβ. In this work we hypothesized that Aβ deposition in cortical sulci would show a stronger association with clinical diagnosis compared to gyral Aβ burden as Aβ preferentially accumulates in cerebral sulci, and that this would translate into better prediction of clinical diagnosis of individual subjects.

## MATERIALS AND METHODS

Data used in the preparation of this article were obtained from the Alzheimer's Disease Neuroimaging Initiative (ADNI) database (http://adni.loni.usc.edu). We studied all patients enrolled in ADNI phases 2 and 3 who had amyloid PET imaging available at the time of the analysis in October 2018. All analysis was performed with IRB approval. The ADNI protocol describes all testing performed and the acquisition protocols in depth (http://adni.loni.usc.edu).

### *Anatomic T1-weighted MR image acquisition and processing*

T1 images using a 3T MR were acquired using either accelerated IR-FSPGR or accelerated MPRAGE sequences. The T1 images were segmented using FreeSurfer (version 6.0; surfer.nmr.mgh.harvard.edu) [10]. All segmentations were visually inspected, and those in which the segmentation failed were reprocessed after manually adjusting the white matter and/or brain masks in the FreeSurfer processing pipeline [11]. One subject was excluded from further analysis due to consistent failure of accurate segmentation which could not be remedied by editing the white matter or brain mask. The cortical regions of interest used in the analysis were: 1) Frontal: caudal middle frontal, lateral orbital frontal, medial orbital frontal, pars opercularis, pars orbitalis, pars triangularis, rostral middle frontal, superior frontal, frontal pole; 2) Temporal: middle temporal, superior temporal; 3) Parietal: inferior parietal, precuneus, superior parietal, supramarginal; 4) Cingulate: posterior cingulate, rostral anterior cingulate. Each region of interest was evaluated in the left and right hemispheres, for a total of 34 regions of interest. The regions of interest (ROI) were chosen as they are known to have high test-retest reliability for average cortical SUVr quantitative analysis of amyloid PET in patients with AD [12].

The cortex was separated into sulci and gyri using curvature measurements of the pial surface calculated by FreeSurfer. Vertices on the pial surface which had a positive curvature were labeled as sulci, and

those with a negative curvature were labeled as gyri. Volumetric masks of cortical gyri and sulci were then created for each subject using the FreeSurfer mri_surf2vol tool. In addition, in order to reduce partial volume effects from the amyloid PET images due to cerebral white matter and CSF, only voxels that were in the middle of the cortical ribbon were used for ROI analysis in PET image processing (described in the next section). This was done also using FreeSurfer's mri_surf2vol tool.

*Amyloid PET image acquisition and processing*

PET image acquisition was performed 50–70 min ($4 \times 5$ min frames) after injection of 10 mCi (370 MBq) $\pm$ 10% of florbetapir. The acquired images were centrally processed by ADNI, including spatial alignment, interpolation to a standard voxel size, and smoothing by 8 mm full width at half maximum (described at adni.loni.usc.edu/methods/pet-analysis-method/pet-analysis).

The T1 images were then registered to the amyloid PET images using FSL's FLIRT tool (https://fsl.fmrib.ox.ac.uk/fsl/fslwiki/FLIRT) with the maximization of mutual information cost function. All images passed a visual inspection for accurate registration. Amyloid PET SUVr images were created by normalizing by the average uptake value of the cerebellar white matter, cerebellar gray matter, brainstem, and cerebral white matter [13]. For the cerebral white matter, a modified mask was created by eroding the mask by 2 mm, in order to reduce partial volume effects between the white matter and adjacent gray matter of the cortex and subcortical gray matter. Finally, the average SUVr of the gyrus and sulcus of each cortical region of interest was calculated.

*Receiver operating characteristic (ROC) curve analysis*

An ROC analysis was performed to evaluate differences in sensitivity/specificity for cognitively unimpaired (NC)/impaired (MCI + AD combined) groups using amyloid PET SUVr in sulci, gyri, and whole structure (sulci + gyri) in the cortical regions of interest. Optimal thresholds for binary Aβ status (positive/negative) based on sensitivity/specificity were then calculated using Youden's J statistic [14]. The threshold calculated for the whole structure analysis was used to define Aβ positivity.

*Statistical analysis*

Summary statistics were computed for demographics and clinical characteristics.

A linear mixed effects model was used to analyze the relationship between amyloid PET SUVr, diagnostic group, and demographic covariates. Included covariates were sex, age, years of education, and ApoE status (positive or negative for the presence of *APOE4* allele). Note that the linear mixed effects model simultaneously analyzes data across all brain regions from each subject in a single model. The random effect of subject is used to model the resulting correlation in measurements. Joint modeling ensures that the estimates are statistically efficient and, therefore, *p*-values do not need to be subsequently corrected for multiple comparisons as only a single model is fit to the data [15]. See the Supplementary Material for a more detailed explanation of the linear mixed effects model.

Logistic regression models were then used to analyze predictive performance of cognitively unimpaired (NC)/impaired (MCI + AD) using amyloid PET SUVr in sulci, gyri, or whole structure (sulci + gyri), with adjustments for age, sex, years of education, and *APOE4* status. The average SUVr in all cortical regions of interest was used as the measure of Aβ burden. A 10-by-10 fold repeated cross-validation was used. Models were compared using Akaike information criterion (AIC).

All statistical analyses were implemented using R, version 3.4.4.

## RESULTS

719 subjects were included in the analysis, 272 NC, 315 with MCI, and 132 with AD. Demographic and clinical data are presented in Table 1. The Aβ positivity threshold was an average amyloid PET SUVr of 0.86 in the regions of interest (more details on the determination of Aβ positivity threshold can be found later in the Results section). As expected, the proportion of amyloid positive individuals increased with worsening clinical diagnosis. Results of the linear mixed effects model for gyral and sulcal Aβ burden are presented in Tables 2 and 3.

For NC, MCI, and AD subjects, Aβ deposition was greatest in cerebral sulci (Fig. 1). The most significant difference in the pattern of Aβ accumulation between NC individuals and subjects with MCI or AD is the extension of Aβ into the cerebral gyri, particularly in the frontal lobes (Fig. 1).

Table 1
Demographic and clinical information with *p*-values from ANOVA or Chi square analysis

| Characteristic ($n = 163$) | NC | MCI | AD | *p* |
|---|---|---|---|---|
| Number (%) | 272 (38%) | 315 (44%) | 132 (18%) | |
| Age (SD) | 73.1 (SD = 6.0) | 71.9 (SD = 7.3) | 74.4 (SD = 8.2) | 0.002 |
| Females (%) | 151 (52%) | 141 (45%) | 57 (43%) | 0.013 |
| Years of Education (SD) | 16.6 (SD = 2.5) | 16.4 (SD = 2.6) | 15.7 (SD = 2.7) | 0.002 |
| ADAS-Cog 13 (SD) | 8.91 (SD = 4.4) | 15.7 (SD = 6.8) | 31.0 (SD = 8.8) | < 0.001 |
| *APOE4* (%) | 79 (29%) | 162 (51%) | 88 (67%) | <0.001 |
| Females with *APOE4* (% of Females) | 51 (34%) | 74 (52%) | 42 (89%) | 0.31 |
| Males with A*POE* (% of Males) | 28 (23%) | 88 (51%) | 46 (61%) | 0.31 |
| Aβ Positive/Negative (% Positive) | 64/208 (24%) | 177/138 (56%) | 115/17 (87%) | < 0.001 |

Table 2
Linear mixed effects model comparing sulcal amyloid PET SUVr in all ROIs and demographic/clinical information

| | Change in SUVr | Standard Error | *p* |
|---|---|---|---|
| Intercept | 0.934 | 0.009 | < 0.00001 |
| MCI | 0.069 (7.39%) | 0.010 | < 0.00001 |
| AD | 0.159 (17.0%) | 0.013 | < 0.00001 |
| Age | 0.004 (0.428%) | 0.001 | < 0.00001 |
| Female | 0.026 (2.78%) | 0.009 | 0.004 |
| Years of Education | –0.001 (0.107%) | 0.002 | 0.642 |
| *APOE4* | 0.103 (11.0%) | 0.009 | < 0.00001 |

Female and *APOE4* variables indicate effects of these variables in the left caudal anterior cingulate regions, which was the reference region used in the linear mixed effects model.

Table 3
Linear mixed effects model comparing gyral amyloid PET SUVr in all ROIs and demographic/clinical information

| | Change in SUVr | Standard Error | *p* |
|---|---|---|---|
| Intercept | 0.733 | 0.0104 | < 0.00001 |
| MCI | 0.082 (11.2%) | 0.011 | < 0.00001 |
| AD | 0.183 (25.0%) | 0.014 | < 0.00001 |
| Age | 0.004 (0.546%) | 0.001 | < 0.00001 |
| Female | 0.045 (6.14%) | 0.010 | 0.00001 |
| Years of Education | –0.001 (0.136%) | 0.002 | 0.490 |
| *APOE4* | 0.119 (16.2%) | 0.010 | < 0.00001 |

Female and *APOE4* variables indicate effects of these variables in the left caudal anterior cingulate regions, which was the reference region used in the linear mixed effects model.

The results of the linear mixed effects model indicate that gyral and sulcal Aβ SUVr increased with worsening clinical diagnosis; however, there was a greater increase in gyral Aβ in both MCI and AD diagnostic groups (Fig. 2). The increase in Aβ deposition with increasing age was the same in both sulci and gyri (Tables 2 and 3). *APOE* status was associated with an increase in both gyral and sulcal Aβ. In subjects that possessed at least one ε4 allele, there was a SUVr increase of 0.103 or 11.0% ($p \leq 0.00001$) in the sulci and 0.119 or 16.2% in the gyri ($p \leq 0.00001$) (Tables 2 and 3). The linear mixed effects model was run with amyloid positive subjects only (Tables 4 and 5). Statistically significant increases in sulcal amyloid burden were observed in the AD clinical diagnosis group ($p = 0.00036$) and positive *APOE* status ($p = 0.036$). MCI clinical diagnosis in the same analysis was of borderline significance ($p = 0.053$). For gyral measures, statistically significant increases in amyloid burden were found in both MCI ($p = 0.012$) and AD ($p = 0.00003$) clinical diagnosis groups and positive *APOE* status ($p = 0.044$). There was a greater increase in gyral amyloid PET SUVr compared to sulcal amyloid PET SUVr in worsening clinical diagnosis groups and positive *APOE* status.

Comparison of sulcal Aβ deposition between males and females demonstrated that females had a greater average Aβ burden in all sulcal regions ($p = 0.004$) and all gyral regions ($p = 0.00001$) (Tables 2 and 3). Females had an increase in SUVr of 0.026 (2.78%) for sulcal Aβ and 0.045 (6.14%) for gyral Aβ compared to male subjects in our cohort. However, there was no significant interaction between sex and clinical diagnosis in sulci or gyri. Table 6 presents the statistically significant sex differences in Aβ burden at specific gyral and sulcal regions. For all cortical regions except for the right pars opercularis sulcus, females had a greater average Aβ burden compared to males. In the analysis of amyloid positive subjects only, gender was no longer associated with a statistically significant increase in Aβ burden (Tables 4 and 5).

ROC analysis demonstrated that there was no demonstrable difference in the sensitivity/specificity performance for diagnostic group between sulcal and gyral Aβ burden (Fig. 3). The optimal SUVr threshold using Youden's J statistic was 1.07 for sulci (sensitivity 0.59, specificity 0.83), 0.82 for gyri (sensitivity 0.61, specificity 0.82), and 0.86 for whole structure (sensitivity 0.66, specificity 0.76). The area

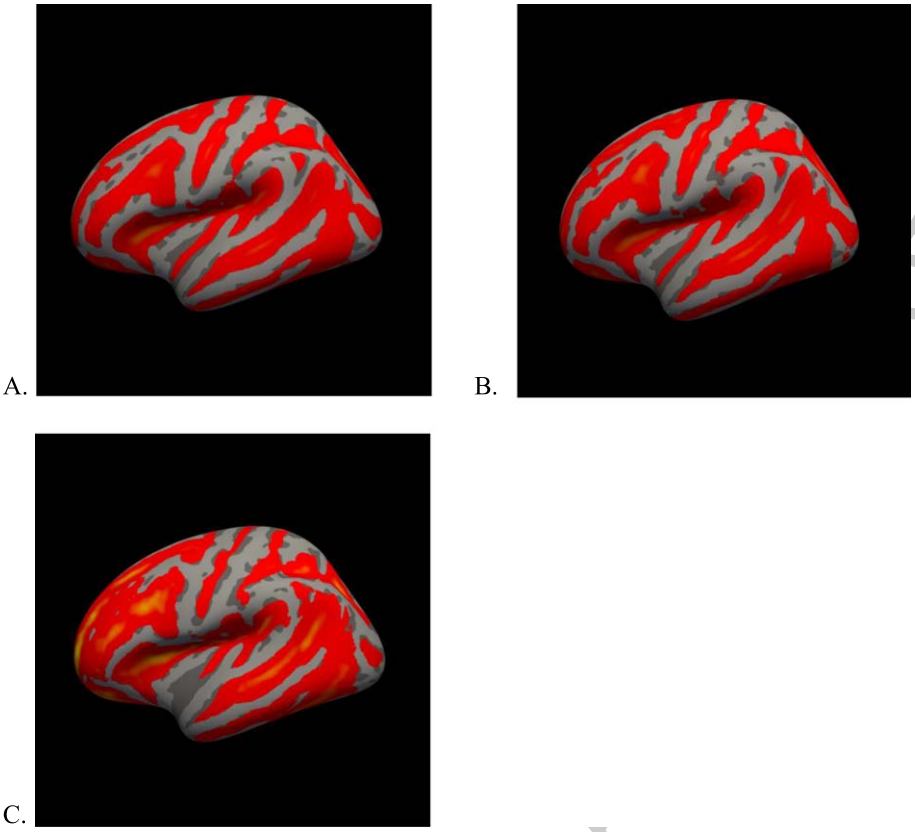


Fig. 1. Surface-based representation of Aβ burden measured by amyloid PET SUVr. In these images, dark grey represents cerebral sulci, light grey represents cerebral gyri, and red/yellow represent areas of greater than the 50th percentile of amyloid PET SUVr distribution, with yellow indicating greater uptake. A) NC subjects. B) MCI subjects. C) AD subjects. In all images, Aβ largely accumulates in the cerebral sulci; with AD, Aβ deposition becomes more prominent in the gyri of the frontal lobe. There was no visually demonstrable difference between males and females in this representation of Aβ burden (separate male/female figures not shown).

Table 4
Linear mixed effects model comparing sulcal amyloid PET SUVr in all ROIs and demographic/clinical information *in amyloid positive subjects only*

| | Change in SUVr | Standard Error | *p* |
|---|---|---|---|
| Intercept | 1.08 | 0.022 | <0.00001 |
| MCI | 0.0428 (4.0%) | 0.022 | 0.053 |
| AD | 0.0840 (7.8%) | 0.023 | 0.00036 |
| Age | 0.00087 (0.081%) | 0.00071 | 0.22 |
| Female | 0.017 (1.6%) | 0.025 | 0.51 |
| Years of Education | 0.0014 (0.13%) | 0.0019 | 0.46 |
| *APOE4* | 0.027 (2.5%) | 0.013 | 0.036 |

Female and *APOE4* variables indicate effects of these variables in the left caudal anterior cingulate regions, which was the reference region used in the linear mixed effects model.

Table 5
Linear mixed effects model comparing gyral amyloid PET SUVr in all ROIs and demographic/clinical information *in amyloid positive subjects only*

| | Change in SUVr | Standard Error | *p* |
|---|---|---|---|
| Intercept | 0.929 | 0.024 | <0.00001 |
| MCI | 0.0601 (6.5%) | 0.024 | 0.012 |
| AD | 0.106 (11.4%) | 0.025 | 0.00003 |
| Age | 0.00060 (0.065%) | 0.00077 | 0.43 |
| Female | 0.0435 (4.7%) | 0.028 | 0.12 |
| Years of Education | 0.00168 (0.18%) | 0.0020 | 0.41 |
| *APOE4* | 0.0282 (3.0%) | 0.014 | 0.044 |

Female and *APOE4* variables indicate effects of these variables in the left caudal anterior cingulate regions, which was the reference region used in the linear mixed effects model.

under the curve was 0.72 for sulci, 0.73 for gyri, and 0.72 for whole structure. Note that this analysis provided the threshold for Aβ positivity used in the analysis (Table 1), which was SUVr of 0.86 for the whole structure (gyri + sulci) in the regions of interest.

Logistic regression analysis did not show any meaningful difference in sensitivity/specificity performance of the sulci, gyri, and whole structure

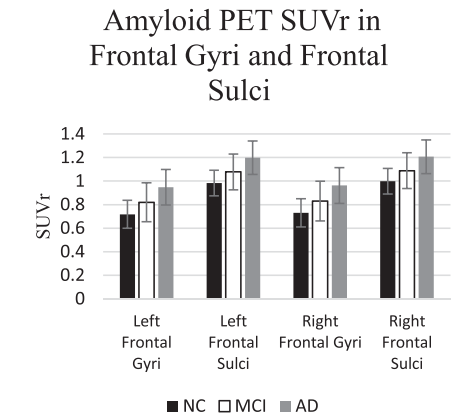


A.

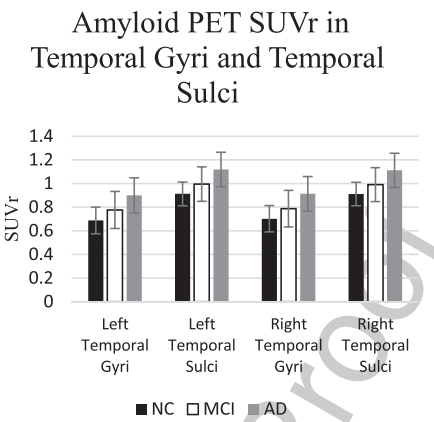


B.

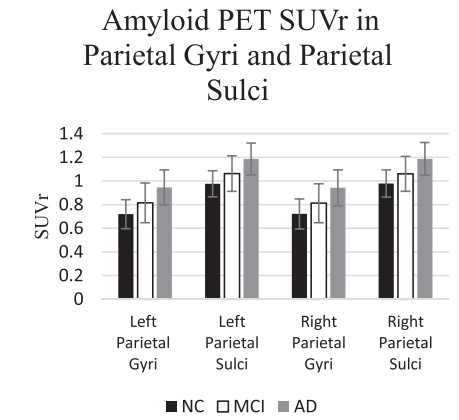


C.

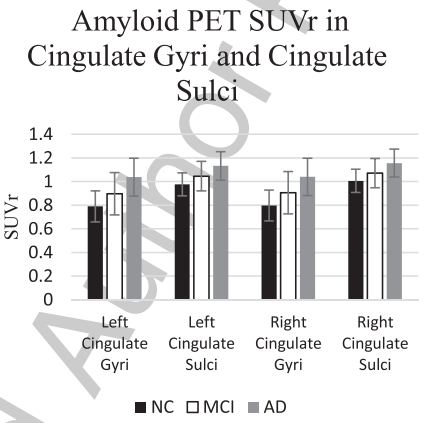


D.

Fig. 2. Amyloid PET SUVr in frontal gyri and frontal sulci (A), temporal gyri and temporal sulci (B), parietal gyri and parietal sulci (C), and cingulate gyri and cingulate sulci (D) each with standard deviation error bars. ROIs included in frontal, temporal, parietal, and cingulate gyri are described in methods.

Table 6
Significant interaction terms ($p < 0.05$) between patient sex and region in the linear mixed effects models

| | Cortical Region | Changes in SUVr Females – Males | $p$ |
|---|---|---|---|
| Gyri | Left frontal pole | 0.046 | < 0.00001 |
| | Left middle temporal | 0.015 | 0.016 |
| | Left pars orbitalis | 0.032 | < 0.00001 |
| | Left pars triangularis | 0.022 | 0.0018 |
| | Left rostral middle frontal | 0.029 | 0.00001 |
| | Left supramarginal | 0.018 | 0.0053 |
| | Right frontal pole | 0.038 | < 0.00001 |
| | Right pars orbitalis | 0.023 | 0.00033 |
| | Right rostral middle frontal | 0.020 | 0.0017 |
| | Right supramarginal | 0.017 | 0.0071 |
| Sulci | Left frontal pole | 0.029 | < 0.00001 |
| | Right frontal pole | 0.020 | 0.0012 |
| | Right pars opercularis | –0.013 | 0.040 |

The standard error for gyral measures was 0.0064 and 0.0062 for sulcal measures.

models. However, AIC analysis demonstrated that the gyri and whole structure models had better fit to the data than the sulci model (better fit models defined as having AIC at least 2 units less than a given model [16]).

## DISCUSSION

In this study, we sought to characterize the pattern of Aβ in cerebral sulci and gyri across the AD spectrum. Our results indicate that in all individuals, regardless of clinical diagnosis, Aβ largely accumulates in cerebral sulci. Interestingly, Aβ accumulation in gyri is more strongly associated with MCI and AD clinical diagnosis groups; however, this association did not lead to increased predictive power in ROC and logistic regression analysis. We also demonstrated

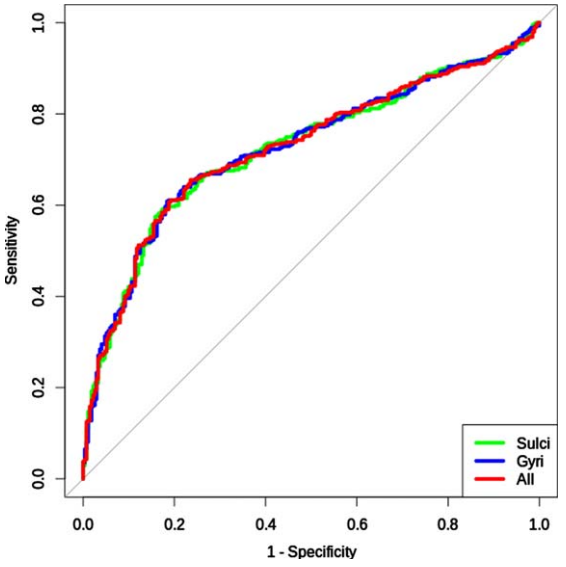


Fig. 3. ROC curves using varying mean amyloid PET SUVr thresholds in sulci, gyri, and whole structure (sulci + gyri) in the cortical regions of interest for classification of cognitively unimpaired (NC) versus impaired (MCI and AD) subjects.

that females have a greater Aβ burden compared to males across the AD spectrum.

Histologically, sulci and gyri are known to have differences in the thickness of supra- and infragranular layers, with sulci containing a larger supragranular layer and gyri containing a larger infragranular layer [3, 17–19]. This anatomical difference is thought to be a result of deformation during cortical folding [20]. Another explanation for this phenomenon could be selective cell death with a bias toward neurons in deeper cortical layers [21]. It is possible that the differential Aβ deposition in sulci and gyri seen in our study is due to these histologic differences.

Although our findings indicate that both gyral and sulcal Aβ increased with worsening clinical diagnosis, this did not translate into increased predictive power in ROC and logistic regression analysis. One of the major challenges in prediction of clinical diagnosis using Aβ identified on PET is the definition of Aβ positivity. A variety of methods have been used in the literature to calculate thresholds including clustering analyses, the 95th percentile, the iterative outlier approach, an absolute cut-off (for example, SUVr > 1.5), the mean + 2 standard deviations (SD) of healthy elderly controls, and the mean + 2 SD of healthy young controls [22]. The choice of methodology for threshold calculation can have a major impact on the definition of Aβ positivity. The literature has reported a wide variation in Aβ positivity rates among cognitive groups with rates of Aβ positivity ranging from 0–47% in NC, 37–72% in MCI, and 68%–100% in AD [22]. There are nearly as many studies that do not identify a relationship between Aβ burden and cognition as there are studies that do identify such a relationship, and rarely do these studies demonstrate a strong relation with heterogenous cohorts [22].

Successful methods for predicting individuals who are likely to experience cognitive decline incorporate multiple factors including imaging, CSF biomarkers, *APOE* status, and a variety of clinical tests [23–27]. In many of these studies, amyloid PET imaging is an integral measure [28]. One study of 564 NC individuals found that patients with elevated Aβ had a greater risk for progression to MCI or dementia (HR, 1.6, 95% CI, 0.9–2.8) [29]. NC individuals with elevated brain Aβ also score worse on the Preclinical Alzheimer Cognitive Composite (PACC) at four year follow up, indicating subtle cognitive decline [30]. Amyloid PET imaging has been shown to be an independent predictor of cognitive decline as early as 6.6 years in advance of cognitive decline [31]. Another study was able to predict the time to conversion from MCI to AD [32]. Separating Aβ by sulci and gyri could be incorporated into these methods and potentially improve the accuracy of cognitive decline prediction.

Previous studies have evaluated the pattern of gyrification in the cortex and its possible relation to AD symptomatology [7, 33–35]. In these studies, abnormalities in global sulcal index and sulcal width have been associated with cognitive decline, possibly related to higher Aβ [36]. This provides another possible course of further analysis—the relationship between Aβ pathology and patterns of gyrification.

In addition to differences in the anatomical distribution of Aβ, there is an unequal distribution of AD across gender groups. Females compose approximately 2/3 of those diagnosed with AD and they suffer more rapid cognitive decline in the context of AD [37]. Data from the Framingham Study found that the lifetime risk of AD for a male was 6.3% (95% CI 3.9 to 8.7) whereas the risk of AD in a female was 12% (95% CI, 9.2 to 14.8) [6]. Another investigation demonstrated that women are at greater risk of developing AD with an odds ratio of 1.56 (95% CI, 1.16–2.10) [39]. Interestingly, one of the most significant relationships between Aβ burden and cognition has been seen in female populations but not male populations [40]. We found that females had greater gyral and sulcal Aβ accumulation compared to males (Tables 2 and 3). When viewed as a percentage, the

increase in gyral Aβ is more than twice as great as the increase in sulcal Aβ (6.14% versus 2.78%). Furthermore, the interaction terms between sex and regional Aβ burden in the linear mixed effects model demonstrates that the predominant regions with statistically significant differences between males and females were in the frontal gyri, with females having a greater Aβ burden in these regions; the only statistically significant region where females did not have a greater Aβ burden than males was the right pars opercularis sulcus (Table 6). Elevated brain Aβ in females could help explain the unequal distribution of AD across genders. Although elevated Aβ accumulation can be identified in NC individuals, the presence of abnormal Aβ remains a major risk factor for cognitive decline [23–26, 28]. Furthermore, global Aβ measures have been inversely correlated to specific cognitive scoring assessments [41, 42]. In contrast, other studies have indicated that specific patterns of high Aβ deposition in regions such as the inferior temporal lobe, striatum, cingulate gyrus, precuneus, or frontal lobe correlate more strongly with clinical diagnosis or that the chronicity of Aβ plaques may play a role in abnormal cognition or rapid cognitive decline [42–47].

The pathologic basis for why females are more susceptible to AD has been explored by other work [48, 49]. In AD, excessive neuroinflammation is frequently cited as a dysregulated mechanism that contributes to disease progression [50]. In this hypothesis, chronic neuroinflammation results in pathologic cytokine production which in turn induces Aβ production [50]. Females have been found to have greater inflammatory dysregulation compared to men [48, 49]. Moreover, microglia, the most common neuroimmune cells, are found in greater numbers in females, possibly generating a greater neuroinflammatory response [48, 49]. The difference in risk profile between males and females could also be attributable to protective estrogenic action in mitochondria that wanes with age [51].

*APOE4* status and age are also well known to confer a significant risk of AD. Individuals with ε4/4 genotype have a 10-fold increase in risk (95% CI, 3.6–35.2) and those with ε3/4 genotype have a 1.7 fold higher risk (95% CI, 1.0–2.9) [52]. In our study, subjects with at least one ε4 allele had a SUVr increase of 0.103 (11.0%) in the sulci and 0.119 (16.2%) in the gyri. After the age of 65, it is estimated that one's risk of AD doubles every 5 years and after the age of 85, AD may affect as much as 1/3$^{rd}$ of the population [53, 54]. In terms of Aβ burden, every year of age beyond the average age of a NC subject in our study increased sulcal and gyral SUVr by 0.004 (0.428% in sulci and 0.546% in gyri). If this cross-sectional data were applied over 5 years, it would represent an increase in 2.14% for sulci and 2.73% in gyri. Although these covariates have been discussed individually, it is important to remember that demographic and genetic factors often work in synergy to accelerate cognitive decline [25].

In contrast to the finding of elevated Aβ accumulation in females and with increasing age in the analysis of all subjects (amyloid positive plus amyloid negative), demographic variables were no longer associated with higher Aβ burden in the amyloid positive only cohort. In both the sulci and gyri, there was no statistically significant elevation in Aβ burden with increasing age or female gender when examining the amyloid positive group alone. This could indicate that once defined as amyloid positive, these factors do not significantly contribute to any further amyloid accumulation. We were unable to find a study with similar results in our literature search. It is well understood that amyloid positivity on PET is a major risk factor for progression to MCI or AD, even though cognitively normal patients may have significant brain Aβ accumulation [29, 55, 56]. For example, when compared to amyloid negative subjects, amyloid positive subjects with MCI have been found to have far higher risk of progression to AD (hazard ratio = 3.74, 95% CI = 1.21–11.58) [55]. It is possible that because amyloid positivity confers such a large risk for progression to MCI/AD and that the average age in our sample was over the age of 70, the relative contributions of sex and age were not major determinants of further Aβ accumulation among those already defined as amyloid positive.

The current study does have limitations. First, although the sample size is 719 individuals, the majority of the subjects are NC ($n = 273$) or MCI ($n = 315$) and a smaller proportion of individuals are diagnosed with AD ($n = 132$). In addition, the unequal distribution in sex across diagnostic groups, with a lower percentage of females in MCI and AD groups compared to NC, could have impacted our results due to a resulting greater variance in the sample population compared to the true variance. A linear modeling analysis of amyloid metrics versus the main effects and interaction between sex and clinical diagnosis was performed, which demonstrated no significant interaction between the terms, and no violation of assumptions of normality or equal variance in the model (see Supplementary Material). Finally, this

study is limited by its cross-sectional nature. However, the large number of subjects strengthens the analysis. More detailed analysis with the inclusion of longitudinal data would be helpful to better quantify the time course of regional Aβ accumulation across the spectrum of AD.

## CONCLUSION

Aβ deposition occurs primarily in cerebral sulci. Aβ deposition in cortical gyri demonstrate a greater association with clinical diagnosis than Aβ deposition in the cortical sulci. However, these differences did not yield improved predictive power for diagnostic group. Females were found to have greater gyral and sulcal Aβ burden compared to males.

## ACKNOWLEDGMENTS

Data collection and sharing for this project was funded by the Alzheimer's Disease Neuroimaging Initiative (ADNI) (National Institutes of Health Grant U01 AG024904) and DOD ADNI (Department of Defense award number W81XWH-12-2-0012). ADNI is funded by the National Institute on Aging, the National Institute of Biomedical Imaging and Bioengineering, and through generous contributions from the following: AbbVie, Alzheimer's Association; Alzheimer's Drug Discovery Foundation; Araclon Biotech; BioClinica, Inc.; Biogen; Bristol-Myers Squibb Company; CereSpir, Inc.; Cogstate; Eisai Inc.; Elan Pharmaceuticals, Inc.; Eli Lilly and Company; EuroImmun; F. Hoffmann-La Roche Ltd and its affiliated company Genentech, Inc.; Fujirebio; GE Healthcare; IXICO Ltd.; Janssen Alzheimer Immunotherapy Research & Development, LLC.; Johnson & Johnson Pharmaceutical Research & Development LLC.; Lumosity; Lundbeck; Merck & Co., Inc.; Meso Scale Diagnostics, LLC.; NeuroRx Research; Neurotrack Technologies; Novartis Pharmaceuticals Corporation; Pfizer Inc.; Piramal Imaging; Servier; Takeda Pharmaceutical Company; and Transition Therapeutics. The Canadian Institutes of Health Research is providing funds to support ADNI clinical sites in Canada. Private sector contributions are facilitated by the Foundation for the National Institutes of Health (http://www.fnih.org). The grantee organization is the Northern California Institute for Research and Education, and the study is coordinated by the Alzheimer's Therapeutic Research Institute at the University of Southern California. ADNI data are disseminated by the Laboratory for Neuro Imaging at the University of Southern California.

Research reported in this publication was supported by the National Cancer Institute of the National Institutes of Health under award numbers: 1U24CA199374-01, R01CA202752-01A1, R01CA 208236-01A1, R01 CA216579-01A1, R01 CA2205 81-01A1, 1U01 CA239055-01, 1U01CA248226-01, 1U54CA254566-01, National Heart, Lung and Blood Institute 1R01HL15127701A1, National Institute for Biomedical Imaging and Bioengineering 1R43EB02 8736-01, National Center for Research Resources under award number 1 C06 RR12463-01, VA Merit Review Award IBX004121A from the United States Department of Veterans Affairs Biomedical Laboratory Research and Development Service, The DoD Breast Cancer Research Program Breakthrough Level 1 Award W81XWH-19-1-0668, The DOD Prostate Cancer Idea Development Award (W81XWH-15-1-0558, W81XWH-20-1-0851), The DOD Lung Cancer Investigator-Initiated Translational Research Award (W81XWH-18-1-0440), The DOD Peer Reviewed Cancer Research Program (W81XWH-16-1-0329), The Kidney Precision Medicine Project (KPMP) Glue Grant 5T32 DK747033, CWRU Nephrology Training Grant, Neptune Career Development Award, The Ohio Third Frontier Technology Validation Fund, The Wallace H. Coulter Foundation Program in the Department of Biomedical Engineering and The Clinical and Translational Science Award Program (CTSA) at Case Western Reserve University.

The content is solely the responsibility of the authors and does not necessarily represent the official views of the National Institutes of Health, the U.S. Department of Veterans Affairs, the Department of Defense, or the United States Government.

Authors' disclosures available online (https://www.j-alz.com/manuscript-disclosures/21-0308r2).

## SUPPLEMENTARY MATERIAL

The supplementary material is available in the electronic version of this article: https://dx.doi.org/10.3233/JAD-210308.

## REFERENCES

[1] Clinton J, Roberts GW, Gentleman SM, Royston MC (1993) Differential pattern of β-amyloid protein deposition within

cortical sulci and gyri in Alzheimer's disease. *Neuropathol Appl Neurobiol* **19**, 277-281.

[2] Gentleman SM, Allsop D, Bruton CJ, Jagoe R, Polak JM, Roberts GW (1992) Quantitative differences in the deposition of βA4 protein in the sulci and gyri of frontal and temporal isocortex in Alzheimer's disease. *Neurosci Lett* **136**, 27-30.

[3] Douaud G, Groves AR, Tamnes CK, Westlye LT, Duff EP, Engvig A, Walhovd KB, James A, Gass A, Monsch AU, Matthews PM, Fjell AM, Smith SM, Johansen-Berg H (2014) A common brain network links development, aging, and vulnerability to disease. *Proc Natl Acad Sci U S A* **111**, 17648-17653.

[4] Chance SA, Tzotzoli PM, Vitelli A, Esiri MM, Crow TJ (2004) The cytoarchitecture of sulcal folding in Heschl's sulcus and the temporal cortex in the normal brain and schizophrenia: Lamina thickness and cell density. *Neurosci Lett* **367**, 384-388.

[5] Fischer VW, Siddiqi A, Yusufaly Y (1990) Altered angioarchitecture in selected areas of brains with Alzheimer's disease. *Acta Neuropathol (Berl)* **79**, 672-679.

[6] McKenzie JE, Gentleman SM, Royston MC, Edwards RJ, Roberts GW (1992) Quantification of plaque types in sulci and gyri of the medial frontal lobe in patients with Alzheimer's disease. *Neurosci Lett* **143**, 23-26.

[7] Liu T, Lipnicki DM, Zhu W, Tao D, Zhang C, Cui Y, Jin JS, Sachdev PS, Wen W (2012) Cortical gyrification and sulcal spans in early stage Alzheimer's disease. *PLoS One* **7**, e31083.

[8] Im K, Lee J-M, Seo SW, Hyung Kim S, Kim SI, Na DL (2008) Sulcal morphology changes and their relationship with cortical thickness and gyral white matter volume in mild cognitive impairment and Alzheimer's disease. *Neuroimage* **43**, 103-113.

[9] Jack CR, Bennett DA, Blennow K, Carrillo MC, Dunn B, Haeberlein SB, Holtzman DM, Jagust W, Jessen F, Karlawish J, Liu E, Molinuevo JL, Montine T, Phelps C, Rankin KP, Rowe CC, Scheltens P, Siemers E, Snyder HM, Sperling R (2018) NIA-AA Research Framework: Toward a biological definition of Alzheimer's disease. *Alzheimers Dement* **14**, 535-562.

[10] Fischl B (2012) FreeSurfer. *Neuroimage* **62**, 774-781.

[11] McCarthy CS, Ramprashad A, Thompson C, Botti J-A, Coman IL, Kates WR (2015) A comparison of FreeSurfer-generated data with and without manual intervention. *Front Neurosci* **9**, 379.

[12] Landau SM, Mintun MA, Joshi AD, Koeppe RA, Petersen RC, Aisen PS, Weiner MW, Jagust WJ (2012) Amyloid deposition, hypometabolism, and longitudinal cognitive decline. *Ann Neurol* **72**, 578-586.

[13] Landau SM, Fero A, Baker SL, Koeppe R, Mintun M, Chen K, Reiman EM, Jagust WJ (2015) Measurement of longitudinal β-amyloid change with 18F-Florbetapir PET and standardized uptake value ratios. *J Nucl Med* **56**, 567-574.

[14] Youden WJ (1950) Index for rating diagnostic tests. *Cancer* **3**, 32-35.

[15] Bernal-Rusiel JL, Greve DN, Reuter M, Fischl B, Sabuncu MR (2013) Statistical analysis of longitudinal neuroimage data with linear mixed effects models. *Neuroimage* **0**, 249-260.

[16] Burnham KP, Anderson DR (2004) Multimodel inference: Understanding AIC and BIC in model selection. *Sociol Methods Res* **33**, 261-304.

[17] Wagstyl K, Ronan L, Whitaker KJ, Goodyer IM, Roberts N, Crow TJ, Fletcher PC (2016) Multiple markers of cortical morphology reveal evidence of supragranular thinning in schizophrenia. *Transl Psychiatry* **6**, e780.

[18] von economo C, Parker S (1929) The cytoarchitectonics of the human cerebral cortex. *J Anat* **63**, 389.

[19] Bok S (1959) *Histonomy of the cerebral cortex*, Elsevier Pub Co.

[20] Borrell V (2018) How cells fold the cerebral cortex. *J Neurosci* **38**, 776-783.

[21] Hilgetag CC, Barbas H (2006) Role of mechanical factors in the morphology of the primate cerebral cortex. *PLoS Comput Biol* **2**, e22.

[22] Chételat G, La Joie R, Villain N, Perrotin A, de La Sayette V, Eustache F, Vandenberghe R (2013) Amyloid imaging in cognitively normal individuals, at-risk populations and preclinical Alzheimer's disease. *Neuroimage Clin* **2**, 356-365.

[23] Davatzikos C, Bhatt P, Shaw LM, Batmanghelich KN, Trojanowski JQ (2011) Prediction of MCI to AD conversion, via MRI, CSF biomarkers, and pattern classification. *Neurobiol Aging* **32**, 2322.e19-27.

[24] Shaffer JL, Petrella JR, Sheldon FC, Choudhury KR, Calhoun VD, Coleman RE, Doraiswamy PM, For the Alzheimer's Disease Neuroimaging Initiative (2013) Predicting cognitive decline in subjects at risk for Alzheimer disease by using combined cerebrospinal fluid, MR imaging, and PET biomarkers. *Radiology* **266**, 583-591.

[25] Mormino EC, Papp KV (2018) Amyloid accumulation and cognitive decline in clinically normal older individuals: Implications for aging and early Alzheimer's disease. *J Alzheimers Dis* **64**, S633-S646.

[26] Baker JE, Lim YY, Pietrzak RH, Hassenstab J, Snyder PJ, Masters CL, Maruff P (2016) Cognitive impairment and decline in cognitively normal older adults with high amyloid-β: A meta-analysis. *Alzheimers Dement (Amst)* **6**, 108-121.

[27] Li K, Chan W, Doody RS, Quinn J, Luo S (2017) Prediction of conversion to Alzheimer's disease with longitudinal measures and time-to-event data. *J Alzheimers Dis* **58**, 361-371.

[28] Rowe CC, Bourgeat P, Ellis KA, Brown B, Lim YY, Mulligan R, Jones G, Maruff P, Woodward M, Price R, Robins P, Tochon-Danguy H, O'Keefe G, Pike KE, Yates P, Szoeke C, Salvado O, Macaulay SL, O'Meara T, Head R, Cobiac L, Savage G, Martins R, Masters CL, Ames D, Villemagne VL (2013) Predicting Alzheimer disease with β-amyloid imaging: Results from the Australian imaging, biomarkers, and lifestyle study of ageing. *Ann Neurol* **74**, 905-913.

[29] Petersen RC, Wiste HJ, Weigand SD, Rocca WA, Roberts RO, Mielke MM, Lowe VJ, Knopman DS, Pankratz VS, Machulda MM, Geda YE, Jack CR (2016) Association of elevated amyloid levels with cognition and biomarkers in cognitively normal people from the community. *JAMA Neurol* **73**, 85-92.

[30] Donohue MC, Sperling RA, Petersen R, Sun C-K, Weiner MW, Aisen PS (2017) Association between elevated brain amyloid and subsequent cognitive decline among cognitively normal persons. *JAMA* **317**, 2305-2316.

[31] Roe CM, Fagan AM, Grant EA, Hassenstab J, Moulder KL, Maue Dreyfus D, Sutphen CL, Benzinger TLS, Mintun MA, Holtzman DM, Morris JC (2013) Amyloid imaging and CSF biomarkers in predicting cognitive impairment up to 7.5 years later. *Neurology* **80**, 1784-1791.

[32] Thung K-H, Yap P-T, Adeli E, Lee S-W, Shen D (2018) Conversion and time-to-conversion predictions of mild

cognitive impairment using low-rank affinity pursuit denoising and matrix completion. *Med Image Anal* **45**, 68-82.

[33] Liu T, Sachdev PS, Lipnicki DM, Jiang J, Cui Y, Kochan NA, Reppermund S, Trollor JN, Brodaty H, Wen W (2013) Longitudinal changes in sulcal morphology associated with late-life aging and MCI. *Neuroimage* **74**, 337-342.

[34] Docherty AR, Hagler DJ, Panizzon MS, Neale MC, Eyler LT, Fennema-Notestine C, Franz CE, Jak A, Lyons MJ, Rinker DA, Thompson WK, Tsuang MT, Dale AM, Kremen WS (2015) Does degree of gyrification underlie the phenotypic and genetic associations between cortical surface area and cognitive ability? *Neuroimage* **106**, 154-160.

[35] Cai K, Xu H, Guan H, Zhu W, Jiang J, Cui Y, Zhang J, Liu T, Wen W (2017) Identification of early-stage Alzheimer's disease using sulcal morphology and other common neuroimaging indices. *PLoS One* **12**, e0170875.

[36] Fan L-Y, Tzen K-Y, Chen Y-F, Chen T-F, Lai Y-M, Yen R-F, Huang Y-Y, Shiue C-Y, Yang S-Y, Chiu M-J (2018) The relation between brain amyloid deposition, cortical atrophy, and plasma biomarkers in amnesic mild cognitive impairment and Alzheimer's disease. *Front Aging Neurosci* **10**, 175.

[37] Podcasy JL, Epperson CN (2016) Considering sex and gender in Alzheimer disease and other dementias. *Dialogues Clin Neurosci* **18**, 437-446.

[38] Seshadri S, Wolf PA, Beiser A, Au R, McNulty K, White R, D'Agostino RB (1997) Lifetime risk of dementia and Alzheimer's disease. The impact of mortality on risk estimates in the Framingham Study. *Neurology* **49**, 1498-1504.

[39] Gao S, Hendrie HC, Hall KS, Hui S (1998) The relationships between age, sex, and the incidence of dementia and Alzheimer disease: A meta-analysis. *Arch Gen Psychiatry* **55**, 809-815.

[40] Pike KE, Ellis KA, Villemagne VL, Good N, Chételat G, Ames D, Szoeke C, Laws SM, Verdile G, Martins RN, Masters CL, Rowe CC (2011) Cognition and beta-amyloid in preclinical Alzheimer's disease: Data from the AIBL study. *Neuropsychologia* **49**, 2384-2390.

[41] Jung Y, Whitwell JL, Duffy JR, Strand EA, Machulda MM, Senjem ML, Lowe V, Jack CR, Josephs KA (2014) Amyloid burden correlates with cognitive decline in Alzheimer's disease presenting with aphasia. *Eur J Neurol* **21**, 1040-1043.

[42] Chételat G, Villemagne VL, Pike KE, Ellis KA, Bourgeat P, Jones G, O'Keefe GJ, Salvado O, Szoeke C, Martins RN, Ames D, Masters CL, Rowe CC, Australian Imaging Biomarkers and Lifestyle Study of ageing (AIBL) Research Group (2011) Independent contribution of temporal beta-amyloid deposition to memory decline in the pre-dementia phase of Alzheimer's disease. *Brain* **134**, 798-807.

[43] Grothe MJ, Teipel SJ (2015) Spatial patterns of atrophy, hypometabolism, and amyloid deposition in Alzheimer's disease correspond to dissociable functional brain networks. *Hum Brain Mapp* **37**, 35-53.

[44] Chen Q, Zhao X, Qiao Z, Wang K, Li X, Wang Xi, Chen Y, Zhang Z, Ai L (2018) Spatial patterns of amyloid deposition in Alzheimer's disease patients. *J Nucl Med* **59**, 1638-1638.

[45] Grothe MJ, Barthel H, Sepulcre J, Dyrba M, Sabri O, Teipel SJ, Initiative F the ADN (2017) *In vivo* staging of regional amyloid deposition. *Neurology* **89**, 2031-2038.

[46] Beach TG, Sue LI, Walker DG, Sabbagh MN, Serrano G, Dugger BN, Mariner M, Yantos K, Henry-Watson J, Chiarolanza G, Hidalgo JA, Souders L (2012) Striatal amyloid plaque density predicts Braak neurofibrillary stage and clinicopathological Alzheimer's disease: Implications for amyloid imaging. *J Alzheimers Dis* **28**, 869-876.

[47] Koscik RL, Norton DL, Allison SL, Jonaitis EM, Clark LR, Mueller KD, Hermann BP, Engelman CD, Gleason CE, Sager MA, Chappell RJ, Johnson SC (2019) Characterizing the effects of sex, APOE $\varepsilon$4, and literacy on mid-life cognitive trajectories: Application of information-theoretic model averaging and multi-model inference techniques to the Wisconsin Registry for Alzheimer's Prevention Study. *J Int Neuropsychol Soc* **25**, 119-133.

[48] Hanamsagar R, Bilbo SD (2016) Sex differences in neurodevelopmental and neurodegenerative disorders: Focus on microglial function and neuroinflammation during development. *J Steroid Biochem Mol Biol* **160**, 127-133.

[49] Hall JR, Wiechmann AR, Johnson LA, Edwards M, Barber RC, Winter AS, Singh M, O'Bryant SE (2013) Biomarkers of vascular risk, systemic inflammation, and microvascular pathology and neuropsychiatric symptoms in Alzheimer's disease. *J Alzheimers Dis* **35**, 363-371.

[50] Minter MR, Taylor JM, Crack PJ (2016) The contribution of neuroinflammation to amyloid toxicity in Alzheimer's disease. *J Neurochem* **136**, 457-474.

[51] Viña J, Lloret A (2010) Why women have more Alzheimer's disease than men: Gender and mitochondrial toxicity of amyloid-β peptide. *J Alzheimers Dis* **20**, S527-S533.

[52] Slooter AJC, Cruts M, Kalmijn S, Hofman A, Breteler MMB, Broeckhoven CV, Duijn CM van (1998) Risk estimates of dementia by apolipoprotein E genotypes from a population-based incidence study: The Rotterdam Study. *Arch Neurol* **55**, 964-968.

[53] Jorm AF, Jolley D (1998) The incidence of dementia: A meta-analysis. *Neurology* **51**, 728-733.

[54] Corrada MM, Brookmeyer R, Paganini-Hill A, Berlau D, Kawas CH (2010) Dementia incidence continues to increase with age in the oldest old: The 90+Study. *Ann Neurol* **67**, 114-121.

[55] Ye BS, Kim HJ, Kim YJ, Jung NY, Lee JS, Lee J, Jang YK, Yang JJ, Lee JM, Vogel JW, Na DL, Seo SW (2018) Longitudinal outcomes of amyloid positive versus negative amnestic mild cognitive impairments: A three-year longitudinal study. *Sci Rep* **8**, 5557.

[56] Zhou B, Tanabe K, Kojima S, Teramukai S, Fukushima M, The Alzheimer's Disease Neuroimaging Initiative (2020) Protective factors modulate the risk of beta amyloid in Alzheimer's disease. *Behav Neurol* **2020**, 7029642.